Supplementary Materials: Water and Ion Dynamics in Confined Media: A Multi-Scale Study of the Clay/Water Interface

Patrice Porion [1,*], Ali Asaad [2], Thomas Dabat [2], Baptiste Dazas[2], Alfred Delville [1,*], Eric Ferrage[2], Fabien Hubert[2], Mónica Jiménez-Ruiz[3], Laurent J. Michot[4], Sébastien Savoye[5] and Emmanuel Tertre[2]

1. Materials and Methods used for Studies of Water and Ion Dynamics in Clay System

1.1. Materials

Clay samples used in these studies are either synthetic, like laponite and saponite, or natural like kaolinite, beidellite and vermiculite. Except kaolinite, they all swell in the presence of water. The swelling clays result from the sandwiching of one layer of octahedral metallic oxides (Al or Mg) between two layers of tetrahedral silicon oxides (see Figure S1). Some atomic substitutions of these metallic atoms by less charged atoms induce residual negative charges of the clay platelet neutralized by counterions localized in the interlamellar space between two clay platelets. By contrast, kaolinite is non-swelling clay, resulting from the stacking of platelets each composed from one layer of octahedral aluminum oxides chemically linked to one layer of tetrahedral silicon oxides (see Figure S1).

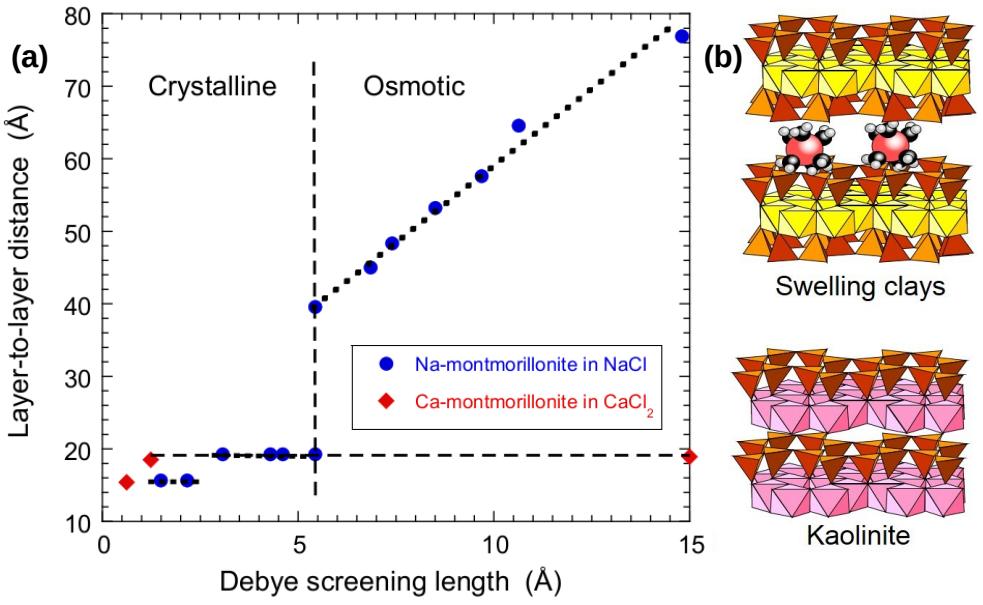

Figure S1. (**a**) X-ray diffraction measurements of the swelling of montmorillonite neutralized either by Na^+ (blue) or by Ca^{2+} (red) counterions and dispersed respectively in NaCl or $CaCl_2$ aqueous solutions. The data are issue from Ref. [1]. (**b**) Structures of kaolinite and swelling clays (montmorillonite, laponite, saponite, beidellite and vermiculite).

The cohesion between two neighboring kaolinite platelets results from a dense network of hydrogen bonds between the hydroxides pertaining to the aluminum oxides of one platelet and the oxygen atoms of the silicon layer from the neighboring platelet. The kaolinite sample was purchased from the Source Clays Mineral Repository at Purdue University (West Lafayette, USA) and purified according to standard procedures [2]. The compacted clay samples were prepared by uniaxial compression of the dry clay powder within a cylindrical container directly used for the NMR measurements [2,3]. Beidellite is a natural swelling clay purchased from the same repository. It was purified according to standard procedure [4] and size separated by centrifugation. Self-supporting films were

prepared by ultrafiltration under nitrogen (3-5 atm) of dilute clay dispersions (10g/L). The resulting film was first dried under nitrogen flux before equilibration with heavy water at fixed chemical potential [5]. Vermiculite used in that study comes from Santa Olalla (Huelva, Spain). In its original form, the centimetric crystals are Mg^+-saturated. The 0.1-0.2 mm particle size fraction was obtained by sonication of centimeter monocrystals immersed in water and centrifugation. Homoionic sample were obtained by saturation with 1M NaCl solutions, followed by dialysis to remove excess NaCl. By contrast with other Na^+-saturated clays (like beidellite, montmorillonite, saponite or laponite), Na^+-saturated vermiculite does not exhibit osmotic swelling. The origin of the transition between crystalline and osmotic swelling is still a subject of debate [6,7] since it may be induced by numerous factors including the valency and water affinity of the counterions [8], the electric charge of the clay platelets [9] and its localization within the atomic clay network [10,11]. Laponite RD is synthetic hectorite clay purchased from Laporte, Ltd. and was used without any purification. The Li^+ exchanged form was obtained by a sequence of saturations with LiCl solutions and separations by centrifugation before purification by dialysis [12]. The saponite synthetic sample was prepared according to standard procedure [4].

1.2. Methods

1.2.1. Neutron Scattering

The Inelastic Neutron Scattering (INS) spectra were measured at 250 K using the IN1-BeF neutron spectrometer installed at the hot source of the high-flux reactor at the Institute Laue-Langevin (ILL, Grenoble, France). This instrument allows to measure directly Generalized Density of States (GDOS), that is the hydrogen partial density of states in the case of hydrogenated materials, in a energy range from 22 to 600 meV with an energy resolution of $\Delta E/E \sim 5\%$. INS spectra were recorded using two different orientations of the sample holder to analyze precisely movements in the parallel and perpendicular directions to the clay layers. More information about the experimental details and data treatment can be found in the References [13] and [14].

Quasi-Elastic Neutron Scattering (QENS) experiments are also performed on oriented clay samples with well controlled hydration state corresponding to the formation of one or two hydration layers, by using the same three-axial set-up. By contrast, the sample temperature was set at 300 K. The measurements are performed again at Institute Laue-Langevin (ILL, Grenoble, France) by using the cold neutron TAS IN14 instrument. The range of investigated wave numbers Q varies between 0.3 and 2.0 $Å^{-1}$. Because of the large incoherent scattering cross section of hydrogen, the QENS signal is dominated by the self-diffusion of water molecules. More details on these QENS experiments are given in the original paper [15].

1.2.2. Nuclear Magnetic Resonance

Nuclear Magnetic Resonance (NMR) ^2H spectroscopy, relaxation and relaxometry measurements were performed at ICMN (Orléans, France) by using a DSX360 Bruker spectrometer operating at a field of 8.465 T. The NMR spectra were recorded in fast acquisition mode with a sampling time of 0.25 μs, corresponding to a 4 MHz spectral window. The various NMR measurements are performed at room temperature with oriented clay sediments. The spectrometer is equipped with a home-made solenoidal coil, allowing varying the orientation of the clay film into the static magnetic field. With this coil, the complete inversion of the longitudinal magnetization is performed by applying pulse duration of 28 μs. The water content of the sediment is stabilized during the measurements by using a small reservoir of heavy water at fixed water chemical potential and localized outside the NMR detection coil. More details on the specific NMR pulses sequences and coherence pathways used in that study are given in the original paper [5].

The same DSX360 Bruker spectrometer was also used for ^7Li multi-quanta relaxometry measurements for probing the influence of ionic condensation on the local mobility of the

lithium counterions within dense laponite gels [12]. For that purpose, we used a homemade solenoidal probe allowing to record ^{7}Li spectra for any orientation of the gel nematic director by reference with the static magnetic field [16]. In that context, a broad spectral width (100 kHz) was used corresponding to a fast acquisition mode with a sampling time of 10 μs, allowing to detect fast relaxation ($R_2 \leq 10^4\,s^{-1}$) and large quadrupolar residual splitting ($\omega_Q \leq 5 \times 10^4$ rad $\cdot$ s^{-1}). In these experimental conditions, the pulse duration for a complete inversion of the longitudinal magnetization varies between 10 and 15 μs. More details on these multi-quanta relaxometry measurements are given in the original article [12].

^{1}H and ^{7}Li Pulsed-Gradient Spin-Echo (PGSE) attenuation measurements were performed on a Bruker DSX100 spectrometer equipped with micro-imaging specific saddle probes with gradient coils in three perpendicular directions in order to generate magnetic field gradients along any arbitrary direction. Figure S2 illustrates the pulse sequence used in the PGSE attenuation measurements. As displayed in Figure S2, we used a modified simulated-echo sequence [17–19] with bipolar-gradients pair to improve the self-diffusion coefficient measurements. As illustrated in Figure S2, both longitudinal (T_1) and transverse (T_2) relaxation rates limit the use of PGSE attenuation measurements since reliable data requires limited diffusion times ($\Delta \leq 3\,T_1$) as well as focusing-refocusing periods ($\tau \leq T_2$). By using a unique set of time delays (typically δ = 500 ms, Δ = 20 ms and τ = 760 ms), the PGSE attenuation evolves according to a Gaussian propagator [19,20]:

$$E(\vec{G},\Delta) = E(0,\Delta)\,\exp\left[-4\,\pi^2\,q^2\,\vec{e}_G^{\,T}\,\mathbf{D}\,\vec{e}_G\left(\Delta+\frac{3}{2}\tau-\frac{\delta}{6}\right)\right] \quad (1)$$

with $q = \gamma\delta G/\pi$, where γ is the gyromagnetic ratio of the NMR nucleus (γ = 2.6752 $\times$ 10^8 rad/s for ^{1}H and 1.037$\times$10^8 rad/s for ^{7}Li), δ is the duration of the applied field gradient, G its strength and $\vec{e}_G$ its direction; **D** is the water self-diffusion tensor, and δ, Δ and τ are time delays illustrated in Figure S2. By measuring the self-diffusion coefficient along 6 non-colinear directions [21], it becomes possible to extract the three eigenvalues and corresponding directors of the tensor **D** describing the mobility of the NMR probes.

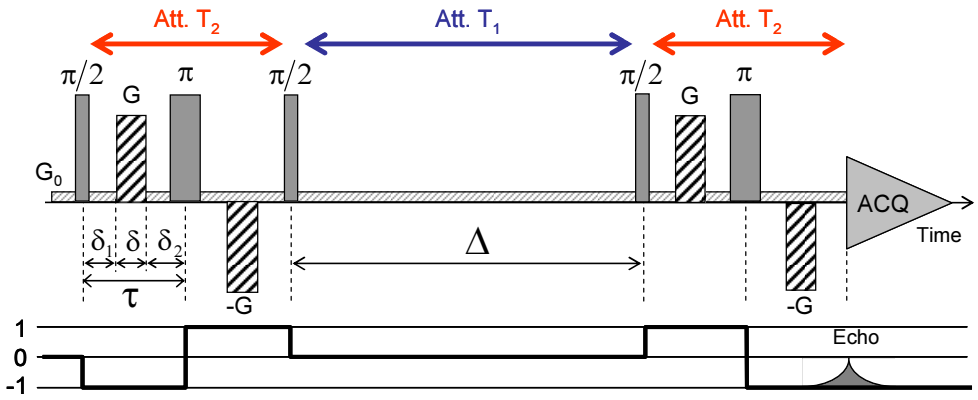

Figure S2. Schematic view of the pulse sequence used to perform NMR Pulsed-Gradient Spin-Echo attenuation measurements in order to probe the influence of clay on the water and Li^+ ions mobility. The red and blue arrows illustrate the time domains corresponding to the transverse (T_2) and longitudinal (T_1) attenuation of the intensity of the NMR signal (see text). Reprinted with permission from Ref. [2]. Copyright (2018) American Chemical Society.

The same Bruker DSX100 spectrometer was used to probe the time-evolution of the ^{1}H concentration profiles during the exchange between water saturated kaolinite sample and heavy water added on the top of the sediment [2] by using Magnetic Resonance Imaging. Figure S3 illustrates the MRI pulse sequence used for these measurements. The field gradient G_Z used to encode the clay sample is oriented parallel to the cylindrical

axis of the sample holder, thus coinciding with its compression axis (see Section 1.1). The initial encoding period ($\delta/2$) is followed by an inversion pulse (noted π) and the same field Gradient G_Z is applied during the evolution period δ=2.56 ms with a simultaneous acquisition. This sequence is used to generate an echo of the NMR signal after a period $\delta/2$, leading to a noticeable attenuation ($\exp[-\delta/(2T_2)] \approx 0.34$) of the NMR signal of the confined water molecules. By contrast, bulk water is not affected by that attenuation, because of the large difference between the corresponding transverse relaxation times ($T_2 \approx 3$ s for bulk water and $T_2 \approx 1.2$ ms for these confined water molecules [2]). The acquisition period (δ) is divided in 256 elementary steps, leading in the same number of elementary sheets in the spatial image obtained by Fourier transform of the time-dependent NMR signal. More details are given in the original paper [2].

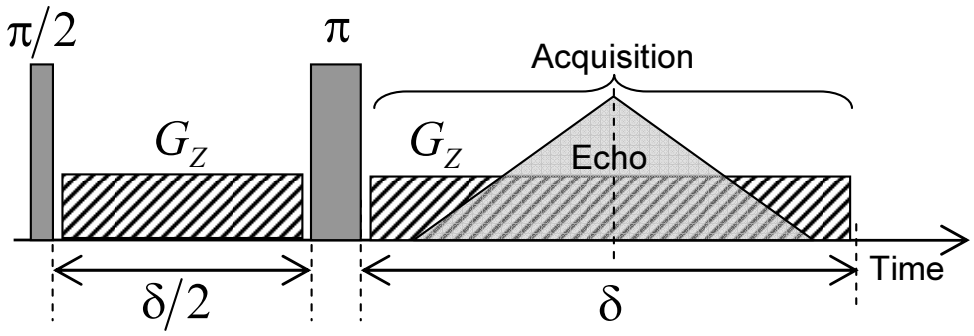

Figure S3. Schematic view of the pulse sequence used to perform Magnetic Resonance Imaging of the water concentration profiles within hydrated kaolinite sediments. Reprinted with permission from Ref. [2]. Copyright (2018) American Chemical Society.

1.2.3. Macroscopic Diffusion Experiments

The Ca^{2+}/Na^{+} and Ca^{2+}/Sr^{2+} exchanges between interlayer space of vermiculite and bulk water was measured by using a macroscopic disk (5 mm in diameter, 0.6-0.7 mm in thickness) of Ca^{2+}-saturated vermiculite, placed between two Teflon plates held by stainless steel clamps and immersed in aqueous NaCl or $SrCl_2$ solutions of known volume (250 mL). In order to probe the Ca^{2+}/Na^{+} and Ca^{2+}/Sr^{2+} exchange mechanisms, various salt concentrations were used, i.e., (3×10^{-3}, 5×10^{-2}, 1×10^{-1} and 1 M NaCl) and (3×10^{-5}, 2×10^{-4}, 1×10^{-2} M $SrCl_2$) respectively. The pH of the solution was fairly constant (5.9 ± 0.2) during these Out-Diffusion experiments. The out-diffusion of calcium from the vermiculite interlayer was quantified by measuring the evolution of the Ca^{2+} concentration in the solution as a function of time by collecting small aliquots (15 mL) of the solution. Those aqueous analyses were performed by using an atomic absorption spectrophotometer (Varian AA240FS), by applying standard analytical procedure [22,23].

Macroscopic diffusion of water in compacted porous media media of kaolinite and vermiculite particles was performed in the framework of Through-Diffusion experiments, by measuring the flux of water tracer (HDO) diffusing through compacted samples prepared within rigid cylinders [24,25]. Diameter of the cylindrical porous media was 0.95 cm while their thickness varied from 0.6 to 1 cm depending on the sample. Furthermore, results reported in this study by using such technique were obtained for HDO diffusing along the clay compaction axis. For that purpose, an upstream reservoir was filled with 50 mL of 0.01 M NaCl solution, spiked with HDO at 0.55 M. The downstream reservoir was filled with Milli-Q water. In order to maintain the gradient of HDO concentration between both reservoirs, they were regularly replaced with fresh ones. The HDO concentration was determined by water isotope analysis (LWIA DFT-100 from Los Gatos Research). More details are given in the original paper [25].

Abbreviations

The following abbreviations are used in this manuscript:

GDOS	Generalized Density Of States
INS	Inelastic Neutron Scattering
MRI	Magnetic Resonance Imaging
NMR	Nuclear Magnetic Resonance
PGSE	Pulsed-Gradient Spin-Echo
QENS	Quasi-Elastic Neutron Scattering

References

1. Norrish, K. The swelling of montmorillonite. *Discuss. Faraday Soc.* **1954**, *18*, 120–134. doi:10.1039/DF9541800120.
2. Porion, P.; Ferrage, E.; Hubert, F.; Tertre, E.; Dabat, T.; Faugère, A.M.; Condé, F.; Warmont, F.; Delville, A. Water mobility within compacted clay samples: Multi-scale analysis exploiting ^{1}H NMR Pulsed Gradient Spin Echo and Magnetic Resonance Imaging of water density profiles. *ACS Omega* **2018**, *3*, 7399–7406. doi:10.1021/acsomega.8b01083.
3. Dabat, T.; Porion, P.; Hubert, F.; Paineau, E.; Dazas, B.; Grégoire, B.; Tertre, E.; Delville, A.; Ferrage, E. Influence of preferred orientation of clay particles on the diffusion of water in kaolinite porous media at constant porosity. *Appl. Clay Sci.* **2020**, *184*, 105354. doi:10.1016/j.clay.2019.105354.
4. Michot, L.J.; Bihannic, I.; Porsch, K.; Maddi, S.; Baravian, C.; Mougel, J.; Levitz, P. Phase diagrams of Wyoming Na-montmorillonite clay. Influence of particle anisotropy. *Langmuir* **2004**, *20*, 10829–10837. doi:10.1021/la0489108.
5. Porion, P.; Faugère, A.M.; Delville, A. Structural and dynamical properties of water molecules confined within clay sediments probed by deuterium NMR spectroscopy, multiquanta relaxometry, and two-time stimulated echo attenuation. *J. Phys. Chem. C* **2014**, *118*, 20429–20444. doi:10.1021/jp506312q.
6. Delville, A. Toward a detailed molecular analysis of the long-range swelling gap of charged rigid lamellae dispersed in water. *J. Phys. Chem. C* **2012**, *116*, 818–825. doi:10.1021/jp208662y.
7. Shen, X.; Bourg, I.C. Molecular dynamics simulations of the colloidal interaction between smectite clay nanoparticles in liquid water. *J. Colloid Interface Sci.* **2021**, *584*, 610–621. doi:10.1016/j.jcis.2020.10.029.
8. Delville, A.; Gasmi, N.; Pellenq, R.J.M.; Caillol, J.M.; Van Damme, H. Correlations between the stability of charged interfaces and ionic exchange capacity: A Monte Carlo study. *Langmuir* **1998**, *14*, 5077–5082. doi:10.1021/la9802872.
9. Pellenq, R.J.M.; Caillol, J.M.; Delville, A. Electrostatic attraction between two charged surface: A (N,V,T) Monte Carlo simulation. *J. Phys. Chem. B* **1997**, *101*, 8584–8594. doi:10.1021/jp971273s.
10. Meyer, S.; Delville, A. (N,V,T) Monte Carlo study of the electrostatic forces between charged lamellae: Influence of surface charge localization. *Langmuir* **2001**, *17*, 7433–7438. doi:10.1021/la0108508.
11. Dzene, L.; Verron, H.; Delville, A.; Michot, L.J.; Robert, J.L.; Tertre, E.; Hubert, F.; Ferrage, E. Influence of tetrahedral layer charge on the fixation of cesium in synthetic smectite. *J. Chem. Phys. C* **2017**, *121*, 23422–23435. doi:10.1021/acs.jpcc.7b06308.
12. Porion, P.; Faugère, A.M.; Delville, A. Long-time scale ionic dynamics in dense clay sediments measured by the frequency variation of the ^{7}Li multiple-quantum NMR relaxation rates in relation with a multiscale modeling. *J. Phys. Chem. C* **2009**, *113*, 10580–10597. doi:10.1021/jp9007625.
13. Jiménez-Ruiz, M.; Ferrage, E.; Blanchard, M.; Fernandez-Castanon, J.; Delville, A.; Johnson, M.R.; Michot, L.J. Combination of inelastic neutron scattering experiments and ab initio quantum calculations for the study of the hydration properties of oriented saponites. *J. Phys. Chem. C* **2017**, *121*, 5029–5040. doi:10.1021/acs.jpcc.6b11836.
14. Mitchell, P.C.H.; Parker, S.F.; Ramirez-Cuesta, A.J.; Tomkinson, J. *Vibrational Spectroscopy with Neutrons - with Applications in Chemistry, Biology, Materials Science and Catalysis*; World Scientific Publishing Co.: Singapore, 2005.
15. Michot, L.J.; Ferrage, E.; Jiménez-Ruiz, M.; Boehm, M.; Delville, A. Anisotropic features of water and ion dynamics in synthetic Na- and Ca-smectites with tetrahedral layer charge. A combined Quasi-Elastic Neutron-Scattering and Molecular Dynamics simulations study. *J. Phys. Chem. C* **2012**, *116*, 16619–16633. doi:10.1021/jp304715m.
16. Porion, P.; Faugère, A.M.; Delville, A. ^{7}Li NMR spectroscopy and multiquantum relaxation as a probe of the microstructure and dynamics of confined Li^{+} cations: An application to dense clay sediments. *J. Phys. Chem. C* **2008**, *112*, 9808–9821. doi:10.1021/jp8010348.
17. Tanner, J.E. Use of the stimulated echo in NMR diffusion studies. *J. Chem. Phys.* **1970**, *52*, 2523–2526. doi:10.1063/1.1673336.
18. Cotts, R.M.; Hoch, M.J.R.; Sun, T.; Markert, J.T. Pulsed field gradient stimulated echo methods for improved NMR diffusion measurements in heterogeneous systems. *J. Magn. Reson.* **1989**, *83*, 252–266. doi:10.1016/0022-2364(89)90189-3.
19. Callaghan, P.T. *Principles of Nuclear Magnetic Resonance Microscopy*; Clarendon Press: Oxford, UK, 1991.
20. Porion, P.; Al-Mukhtar, M.; Faugère, A.M.; Pellenq, R.J.M.; Meyer, S.; Delville, A. Water self-diffusion within nematic dispersion of nanocomposites: A multiscale analysis of ^{1}H pulsed gradient spin-echo NMR measurements. *J. Phys. Chem. B* **2003**, *107*, 4012–4023. doi:10.1021/jp022161q.
21. Basser, P.J.; Mattiello, J.; LeBihan, D. Estimation of the effective self-diffusion tensor from the NMR spin-echo. *J. Magn. Reson. B* **1994**, *103*, 247–254. doi:10.1006/jmrb.1994.1037.

22. Tertre, E.; Delville, A.; Prêt, D.; Hubert, F.; Ferrage, E. Cation diffusion in the interlayer space of swelling clay minerals – A combined macroscopic and microscopic study. *Geochim. Cosmochim. Acta* **2015**, *149*, 251–267. doi:10.1016/j.gca.2014.10.011.
23. Tertre, E.; Dazas, B.; Asaad, A.; Ferrage, E.; Grégoire, B.; Hubert, F.; Delville, A.; Delay, F. Connecting molecular simulations and laboratory experiments for the study of time-resolved cation-exchange process in the interlayer of swelling clay minerals. *Appl. Clay Sci.* **2021**, *200*, 105913. doi:10.1016/j.clay.2020.105913.
24. Asaad, A.; Hubert, F.; Ferrage, E.; Dabat, T.; Paineau, E.; Porion, P.; Savoye, S.; Gregoire, B.; Dazas, B.; Delville, A.; Tertre, E. Role of interlayer porosity and particle organization in the diffusion of water in swelling clays. *Appl. Clay Sci.* **2021**, *207*, 106089. doi:10.1016/j.clay.2021.106089.
25. Tertre, E.; Savoye, S.; Hubert, F.; Prêt, D.; Dabat, T.; Ferrage, E. Diffusion of water through the dual-porosity swelling clay mineral vermiculite. *Environ. Sci. Technol.* **2018**, *52*, 1899–1907. doi:10.1021/acs.est.7b05343.